

**Novel polyvinylpyrrolidones to improve delivery of poorly-water soluble drugs;
from design to synthesis and evaluation**

Anna I. Niemczyk¹, Adrian C. Williams^{1}, Clare F. Rawlinson-Malone^{1,3}, Wayne Hayes², Barnaby W. Greenland², David Chappell², Olga Khutoryanskaya¹, Peter Timmins³.*

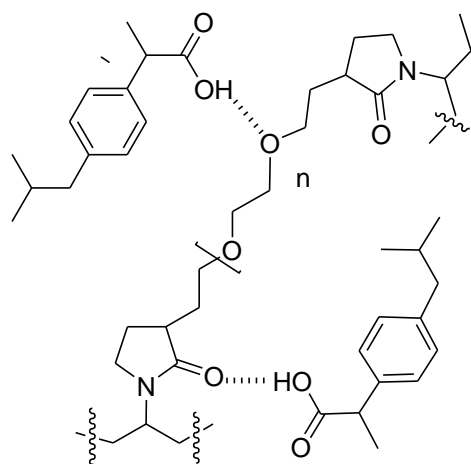
¹School of Pharmacy, University of Reading, Whiteknights, P.O. Box 226, Reading, RG6 6AP, UK

²Department of Chemistry, University of Reading, Whiteknights, P.O. Box 224, Reading, RG6 6AD, UK

³Drug Product Science and Technology, Bristol-Myers Squibb, Reeds Lane, Moreton, Wirral, CH46 1QW, UK

Running title: novel PVP synthesis and evaluation

*Corresponding author: Adrian Williams, School of Pharmacy, University of Reading, Whiteknights, PO Box 226, Reading RG6 6AP, UK. Telephone: +44 118 378 6196. E.mail: a.c.williams@reading.ac.uk



$n = 3 \text{ or } 5$

Abstract

Polyvinylpyrrolidone is a widely used in tablet formulations with the linear form acting as a wetting agent and disintegrant whereas the cross-linked form is a super-disintegrant. We have previously reported that simply mixing the commercial cross-linked polymer with ibuprofen disrupted drug crystallinity with consequent improvements in drug dissolution behavior. In this study, we have designed and synthesized novel cross-linking agents containing a range of oligoether moieties which have then be polymerized with vinylpyrrolidone to generate a suite of novel excipients with enhanced hydrogen-bonding capabilities. The polymers have a porous surface and swell in most common solvents and in water; properties which suggest their value as disintegrants. The polymers were evaluated in simple physical mixtures with ibuprofen as a model poorly-water soluble drug. The results show that the novel PVPs induce the drug to become “X-ray amorphous”, which increased dissolution to a greater extent than that seen with commercial cross-linked PVP. The polymers stabilize the amorphous drug with no evidence for recrystallization seen after 20 weeks storage.

Keywords

Polyvinylpyrrolidone, amorphous, dissolution, poorly-water soluble drugs, hydrogen bonding.

Introduction

Over the last decade, highly non-polar drugs have emerged from discovery groups as a consequence of the drive to improve specificity at novel target sites that are hard to access with traditional compounds with lesser lipophilicities. Inherently poorly-water soluble, these potent compounds present considerable difficulties for enteral delivery and absorption. Indeed, it has been recognized for many years that Biopharmaceutical Classification System (BCS) class II compounds (i.e. those with low aqueous solubility but high permeability¹) can present absorption rate-limiting dissolution in the gastric media, impacting significantly on bioavailability.

An increasingly valuable strategy for improving the bioavailability of this class of active pharmaceutical ingredients is to use an amorphous drug species²⁻³. The glassy amorphous state theoretically has a higher apparent solubility than the crystalline counterpart⁴ because these two morphologies differ in the thermodynamic processes of breaking intermolecular associations during dissolution, i.e. enthalpy, entropy, and free energy⁵. This solid state manipulation can therefore be exploited as a means to achieve significant apparent dissolution rate enhancement. However, due to the inherent instability of the amorphous state, a viable dosage form requires a method of stabilizing this meta-stable state to prevent recrystallization to the more stable, less soluble crystalline form². To this end, one strategy is to disperse amorphous drug in a polymeric matrix or gel. Ideally, the polymer will be robust in order to withstand manufacture processes, will be pharmacologically inert and biocompatible with no appreciable toxicity and will be able to sequester the active pharmaceutical ingredient.

Using differential scanning calorimetry to screen compatibility of ketoprofen with excipients, Mura et al.⁶ reported the loss of the drug melting peak in a simple physical blend with K30 polyvinylpyrrolidone (PVP). In the same year, solid-state interactions in mixtures between ibuprofen and (PVP) were reported by Sekizaki et al⁷; the formation of amorphous ibuprofen in the mixtures was enhanced by elevated storage temperatures, a high weight ratio of PVP and by using lower molecular weight PVP. In our earlier work, we employed cross-linked polyvinylpyrrolidone (PVP-CL) as a carrier in physical mixtures with ibuprofen⁸⁻¹⁰ with results suggesting that disruption of drug crystallinity was facilitated primarily through hydrogen bonding with a

secondary mechanism involving electrostatic/hydrophobic interactions through the ibuprofen benzene ring. Following grinding and mixing, hydrogen-bonding between ibuprofen dimers and linear PVP (Povidone K25) was reported¹¹. In contrast, Di Martino reported no evidence for interaction between ketoprofen and linear PVP K30 after gentle mixing, although powder X-ray diffraction showed that the drug lost crystallinity following 10 months storage¹². More recent studies using different propionic acids with linear PVP K30 have further confirmed our earlier findings that hydrogen bonding and electrostatic interactions are key determinants in the solid-state interactions between ibuprofen and polyvinylpyrrolidones^{13, 14} whilst illustrating the role of relative humidity.

Whilst the mechanisms underpinning the thermodynamic drivers remain unclear, our own previous work using cross-linked PVP and the literature employing linear PVP with aryl propionic acids, shows that inter-molecular hydrogen bonding is the driving force for retention and stabilization of the drug as “X-ray amorphous”; here, we define “X-ray amorphous” as meaning the absence of clear Bragg diffraction peaks from the powder X-ray diffraction pattern, whilst recognizing that this does not *necessarily* mean that the material in question is truly amorphous; it may in fact be nanocrystalline. Thus, through tailoring the molecular composition of cross-linked PVPs by designing functionalized cross-linking agents, the stabilizing properties of the polymer can be optimized. We sought to synthesize novel cross-linking agents where the NVP residues were connected by hydrophilic oligoethers rather than hydrophobic alkane-based residues as in all previous work^{15, 16}. PEG polymers have been used for solid dispersions and potential hydrogen bonding mechanisms have previously been reported¹⁷. We hypothesise that the enhanced hydrogen bonding potential of the oligoethers would further aid disruption of ibuprofen crystallinity when incorporated into pharmaceutical formulations. Herein we report the design, synthesis and pharmaceutical uses of a series of novel polyvinylpyrrolidones built with oligoether cross-linkers of varying polarities at different molar fractions, and demonstrate the ability of these polymers to create stable amorphous delivery systems when simply mixed with the model poorly-water soluble drug ibuprofen.

Experimental Section

Materials

Ibuprofen (IB) was obtained from Wessex Fine Chemicals (Horsham, UK) and commercial cross-linked polyvinylpyrrolidone XL-10 (PVP-CL) was from ISP Technologies Inc. All other reagents were purchased from Sigma-Aldrich Chemical Company (Poole, UK) and were used as received except for *N*-vinylpyrrolidone (NVP) which was freshly distilled prior to use and 2,2' azobisisobutyronitrile (AIBN) which was recrystallized from methanol.

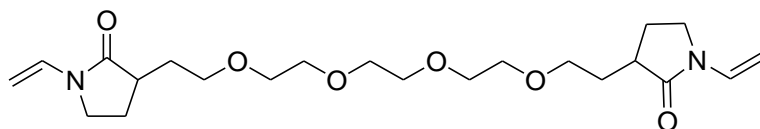
Solvents were also purchased from Sigma-Aldrich Chemical Company (Poole, UK) and were used without purification except; dichloromethane was pre-dried over calcium hydride prior to distillation; tetrahydrofuran (THF) was distilled from sodium and benzophenone prior to use; pyridine was dried over potassium hydroxide prior to distillation; benzene used in polymerization reactions was degassed for 30 minutes prior to use. All glassware was dried overnight in an oven at 120 °C prior to use.

Synthetic methods

Synthesis of cross-linkers

Two novel cross-linking agents were synthesized for subsequent use in polymerization with *N*-vinylpyrrolidone. The cross-linkers were designed to possess appropriate reactivity ratios with the monomer and hence coupled two NVP units with oligoether chains of varying lengths, as illustrated in Figure 1.

A



B

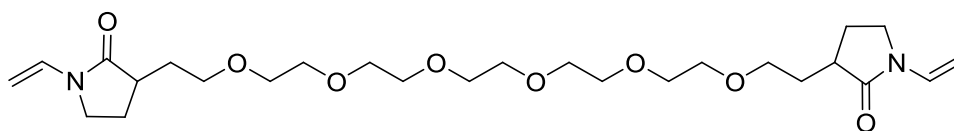


Figure 1. Chemical structure of the novel cross-linking agents designed to polymerize with vinylpyrrolidone and offering differing lengths of oligoether chains. A). 3,3'-(3,6,9,12-Tetraoxatetradecane-1,14-diyl)*bis*(1-vinyl-2-pyrrolidinone); B). 3,3'-(3,6,9,12,15,18-Hexaoxaicosane-1,20-diyl)*bis*(1-vinyl-2-pyrrolidinone).

A stirring solution of 3-(2-hydroxyethyl)-1-vinyl-2-pyrrolidinone (1.25 eq., 11.0 mmol, 1.70 g) in anhydrous *N,N*-dimethylformamide (DMF; 60 mL) under argon and at room temperature was treated with sodium hydride (60% dispersion in mineral oil, 1.38 eq., 12.1 mmol, 0.48 g) followed by tetra-*N*-butylammonium bromide (0.8 mmol, 0.35 g). The reaction mixture was stirred at 70 °C until effervescence ceased at which point (3,6-dioxaoctane-1,8-diyl)*bis*(4-methyl-benzenesulfonate) (4.4 mmol, 2.02 g) was added and stirring was continued for a further 7 hours. Following filtration, the filtrand was washed with successive volumes of dichloromethane (5 × 10 mL) until there was no sign of product *via* TLC. The resulting organic fractions were concentrated *in vacuo* prior to subjecting the crude to flash column chromatography (SiO₂, ethyl acetate/hexane 9:1 v/v) following which 3,3'-(3,6,9,12-tetraoxatetradecane-1,14-diyl)*bis*(1-vinyl-2-pyrrolidinone) was obtained as a pale yellow oil (0.78 g, 1.84 mmol, 42% yield).

Likewise, a stirring solution of 3-(2-hydroxyethyl)-1-vinyl-2-pyrrolidinone (1.25 eq., 8.5 mmol, 1.31 g) in anhydrous DMF (60mL) under argon and at room temperature was treated with sodium hydride (60% dispersion in mineral oil, 1.38 eq., 9.4 mmol, 0.37 g) followed by tetra-*N*-butylammonium bromide (12.5 mol%, 0.27 g). The reaction mixture was stirred at 70 °C until effervescence ceased at which point (3,6,9,12-tetraoxatetradecane-1,14-diyl)*bis*(4-methyl-benzenesulfonate) (3.4mmol, 1.86g) was added and stirring was continued for a further 7 hours. Following filtration the filtrand was washed with successive volumes of dichloromethane (5 × 10mL) until there was no sign of product *via* TLC. The resulting organic fractions were concentrated *in vacuo* prior to subjecting the crude to flash column chromatography (SiO₂, ethyl acetate/hexane 9:1 v/v) following which 3,3'-(3,6,9,12,15,18-hexaoxaicosane-1,20-diyl)*bis*(1-vinyl-2-pyrrolidinone) was obtained as a pale yellow oil (0.71 g, 1.39 mmol, 41% yield).

Polymerization

2,2'-Azobisisobutyronitrile (AIBN; 1 mol%) was weighed into a flame-dried Schlenk tube under argon followed by *N*-vinylpyrrolidinone. The cross-linker (A or B, Table 1) was weighed into a vial and dissolved in benzene before being transferred to the Schlenk tube. The reaction was stirred at room temperature whilst the Schlenk tube was evacuated and purged with argon three times. The resulting colourless solution was stirred magnetically for 15 hours at 60 °C and under argon during which time the viscosity of the generated polymer reached a sufficiently high level to prevent stirring. Once cooled, the tough gel was cut into small pieces and subjected to Soxhlet extraction with chloroform before the polymer was dried in a vacuum oven (50 °C, 10 mmHg, 48 hours). The polymers were then size reduced (planetary ball mill; 1 hour) followed by additional drying in a vacuum oven (50 °C, 10 mmHg, 18 hours) which provided fine white polymer powders that were sieved (Fritsch Vibratory Sieve Shaker, Germany) to recover particle sizes between 30-50µm for subsequent studies, the same size range as the commercial cross-linked polyvinylpyrrolidone (PVP-CL XL10).

The two cross-linking agents were used in different proportions to generate varied cross-linking densities in the novel polymers (Table 1). For simplicity, polymers using the shorter tetra-oligo linker are given the prefix “5” and those synthesised using the longer hexa-oligo linker are prefixed with “7”. To include the varying percentage of cross-linker used in the reactions, the polymers are then designated with either 1, 2.5 or 5%. Thus, 5 PVP 1% is the polymer synthesised using the shorter tetra-oligo cross-linking agent at 1% in the reaction whereas 7 PVP 5% is constructed from the longer hexa-oligo linker included at 5% in the polymerisation reaction.

Cross-linker	Percentage cross-linker used in reaction								
	1.0 wt%			2.5 wt%			5.0 wt%		
	NVP	Benzene	Yield	NVP	Benzene	Yield	NVP	Benzene	Yield
A (short)	8.00g	10.0 mL	7.30g 90.3%	8.00g	10.0 mL	7.16g 87.3%	6.52g	8.1 mL	6.18g 90.2%
B (long)	8.00g	10.0 mL	7.22g 89.4%	8.00g	10.0 mL	7.11g 86.7%	6.52g	8.1 mL	6.24g 91.1%

Table 1. Amounts of reagents used in polymerisation reactions. Cross-linker A (short) is 3,3'-(3,6,9,12-tetraoxatetradecane-1,14-diyl)*bis*(1-vinyl-2-pyrrolidinone); B (long) is 3,3'-(3,6,9,12,15,18-hexaoxaicosane-1,20-diyl)*bis*(1-vinyl-2-pyrrolidinone).

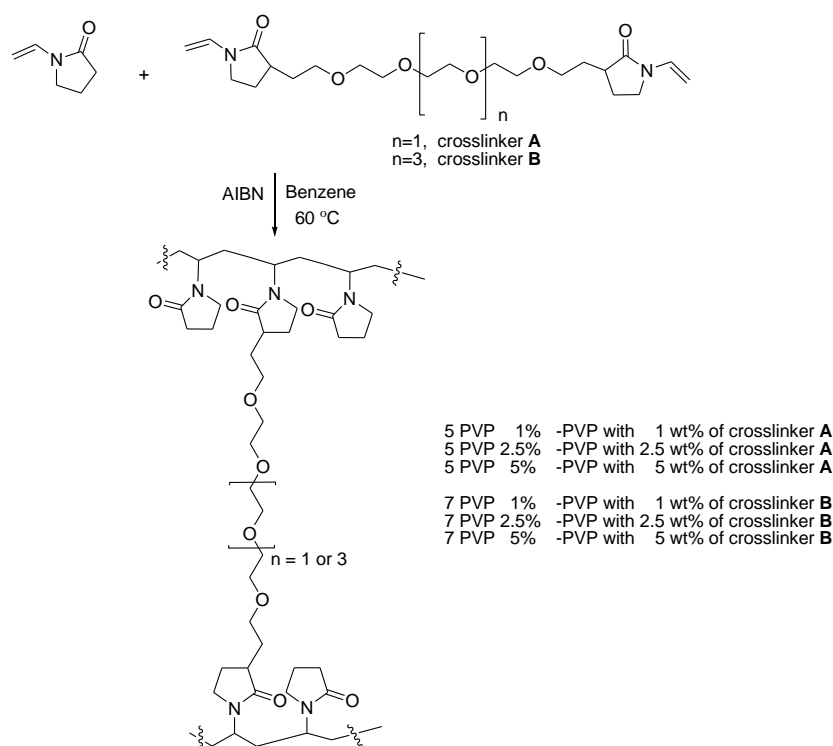


Figure 2. General reaction scheme for synthesis of novel cross-linked polyvinylpyrrolidones

Analytical methods

Prior to polymerization, the novel cross-linking agents were characterized by thin layer chromatography, by ^1H NMR and ^{13}C NMR spectra (Bruker AC250 spectrometer, 250 and 62.5 MHz respectively), using Fourier Transform infrared spectroscopy (Perkin Elmer 1720-X.), and mass spectrometry (Fiscon VG Autospec mass spectrometer with chemical ionization). The results confirmed the structures reported in Figure 1; data can be retrieved as Supporting information and is available free of charge via the internet at <http://pubs.acs.org>.

Illustrating their cross-linked natures, the polymers did not dissolve in common solvents but swelled prodigiously in, for example, dichloromethane, *N,N*-dimethylformamide, methanol and dimethylsulfoxide; thus mass spectrometry and NMR analysis was problematic. The polymers were characterized by their glass transition temperatures detected by differential scanning calorimetry which was calibrated using indium (melting point 156.6°C, ΔH_f 28.4 J/g) and zinc (melting point 419.6°C, ΔH_f 108.2 J/g). Samples (~6 mg) were accurately weighed into pin-holed aluminum pans then heated at 20°C/min to 300°C in a Mettler Toledo DSC 823E under a purge of dry nitrogen gas. The samples were held at 300°C for 1 minute before cooling at 20°C/min to 0°C and then reheated at 20°C/min to 300°C; glass transition temperatures were determined during the second heating cycle, after controlling the thermal history of the polymers.

The surface morphologies of the polymer particles (and physical mixtures of drug:polymers during pharmaceutical evaluation) were visualized using a LEO 145 OVP Scanning Electron Microscope. Samples were mounted onto aluminum stubs using double sided adhesive tape before coating with gold in a high resolution sputter coater (Edwards Sputter Coater S150B).

Infrared spectra of the polymers were collected using a Perkin Elmer Spectrum 100 FT-IR spectrometer equipped with a universal ATR sampling accessory. Typically 100 scans collected at 4 cm⁻¹ were averaged for each polymer. The same parameters were used to analyze drug:polymer mixtures.

Pharmaceutical evaluation

Preparations of physical mixtures

Prior to preparing physical mixtures, both ibuprofen and the novel cross-linked PVPs were sieved (Fritsch Vibratory Sieve Shaker, Germany). The same sieve fraction as that of commercial PVP-CL, namely 30-50 µm, was collected for further use, thus reducing potential variations as a result of differences in polymer particle sizes.

In the case of IB, the sieve fraction 75-180 µm was chosen to eliminate both large aggregates and “fine” particles which would be unfavorable in mixing. Physical mixtures of IB and polymers (novel PVPs and PVP-CL) were prepared containing 30% by weight IB to replicate the optimum drug:polymer ratio identified in our

previous studies with PVP-CL⁶. The batch size was 4g and all samples were mixed for 15 minutes in a sealed container using a Turbula mixer (Glen Creston Ltd, UK). Likewise, controls of IB and polymers alone were treated for 15 minutes in the mixer to parallel any effects arising from attrition. All samples were stored in sealed glass vials before analysis.

The homogeneity of each physical mixture was confirmed. Drug contents in three samples (30 mg) taken randomly from each physical mixture were determined by UV spectroscopy at 222 nm (Varian Cary 50 Bio UV-Visible Spectrophotometer, US) against a calibration curve; measured IB contents were between 29.83-30.06% (theoretical contents 30%), showing that all mixtures were homogeneous.

Dissolution testing

Dissolution testing of the physical mixtures and samples of pure IB (75-180 μm) was carried out using the paddle method (British Pharmacopeia, 2011) under sink conditions in pH 5.5 phosphate buffer at $37\pm 1^\circ\text{C}$ and 50 rpm. Solubility of IB in the buffer at 37°C was 0.55 ± 0.01 mg/mL so samples equivalent to 18 mg of pure IB were transferred to 1000 mL of the dissolution media to ensure sink conditions. Aliquots (4 mL) were withdrawn periodically up to 180 minutes and filtered (Millex-HA, Syringe Driven Filter Unit, 0.45 μm , Fisher Scientific UK) before IB absorbance was measured at 222 nm (Varian Cary 50 Bio UV-Visible Spectrophotometer, US). IB concentrations were calculated from a calibration curve in the same buffer and results are expressed as percentage IB released from the mean of triplicate tests.

Differential scanning calorimetry

DSC analysis of mixtures used a Perkin-Elmer 7 series Thermal Analysis System with nitrogen purge. The calorimeter was calibrated with pure indium (melting point 156.6°C , $\Delta H_f = 28.4$ J/g) and zinc (melting point 419.6°C , $\Delta H_f = 108.2$ J/g). Samples 5 - 10 mg) were accurately weighed then heated from $25 - 95^\circ\text{C}$ at $10^\circ\text{C}/\text{min}$. The data from the thermal profiles was used to indicate drug crystallinity, according to:

$$\text{Percent crystallinity} = \left(\frac{\Delta H}{\Delta H_{\text{IB}} \cdot W} \right) \cdot 100\%$$

Where ΔH is the melting enthalpy of the physical mixture (J/g), ΔH_{IB} is the melting enthalpy of pure ibuprofen (J/g, and assumed to be 100% crystalline) and W is the weight fraction of ibuprofen in the physical mixture (i.e. $W=0.3$). All analyses were in triplicate.

Powder X-ray diffraction

Powder X-ray diffraction (PXRD) patterns were recorded using a D8 Advance Diffractometer (Bruker AXS) operating in Bragg-Brentano (flat plate) geometry under the following conditions: target $\text{CuK}\alpha_1$ ($\lambda = 1.54056\text{\AA}$); voltage 40 kV; current 40 mA. The data were collected from $5-60^\circ 2\theta$ using a step size of $0.010^\circ 2\theta$. The scanned samples were placed in a standard holder and the surface of the material carefully smoothed in order to minimize and zero point error.

Results and discussion

Monomer design and synthesis

Previous work has shown that there is a large difference in reactivity ratios between the vinyl group in NVP and well-studied monomers such as methacrylate and styrene^{18,19}. Thus, attempts to co-polymerize commercial cross-linkers such as ethylene dimethacrylate and divinylbenzene with NVP do not result in random, homogeneously cross-linked co-polymers that are the target of this work.

The problem of the incompatibility of reactivity ratios between NVP and commercial cross-linking monomers has been elegantly overcome by White *et al*^{15,16}. During fundamental studies into the kinetics of NVP polymerizations they produced a novel cross-linker, synthesized by the addition of two equivalents of NVP to 1,6-dibromohexane under basic conditions. The resulting cross-linker, containing two NVP residues, was found to be readily compatible with NVP under photo-initiated free radical polymerization conditions, producing homogeneously cross-linked materials. This approach to synthesizing cross-linked NVP has recently been

exploited by Engström *et al.* to produce supports for solid phase synthesis and water swellable drug delivery systems²⁰⁻²².

Our targeted diNVP cross-linkers were accessed through the addition of the known hydroxy functionalized NPV derivative^{21,22} to either of the commercially available ditosylates (Figure 3). It should be noted that attempts to form oligoether cross-linkers by direct addition of NVP to the ditosylates under basic conditions failed as a consequence of over alkylation of the NVP ring, which led to a complex mixture of cyclic and oligomeric species. In our cross-linkers, both NVP units and the oligoether chains appear to be hydrogen bond active. It was expected that modulating the oligoether chain and the density of cross-linking might additionally affect the number of hydrogen bonding sites and also their accessibility in the PVP network.

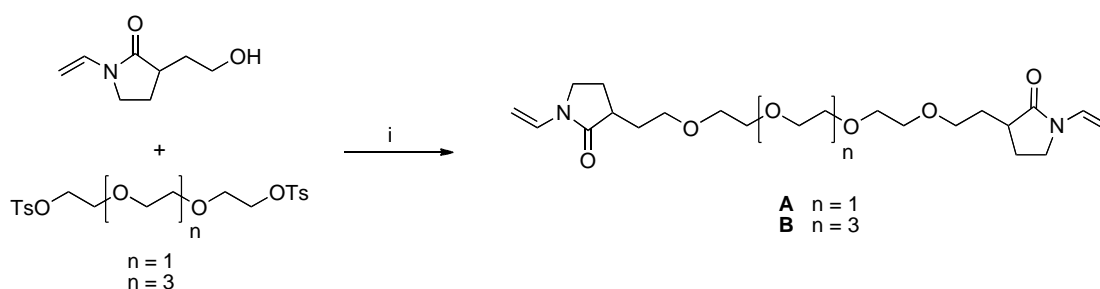


Figure 3. Synthesis of diNVP cross-linkers. Reagents and conditions: i) NaH, DMF, cross-linker A; 42%: cross-linker B; 41% (both isolated as a mixture of diastereomers).

As our cross-linkers are NVP derivatives, they were expected to possess similar reactivity ratios as NVP (as a result of structural similarity) and so co-polymerize easily with NVP without compositional drift. Indeed, the syntheses of our novel PVPs via free radical polymerization succeeded, affording the six polymers (Figure 2) varying in the length of the oligoether chain (PVPs with the shorter and longer oligoether chain were abbreviated as “5 PVP” and “7 PVP”, respectively) and in the density of cross-linking (the cross-linker content in the feed polymerisation mixture were 1, 2.5 or 5 wt%).

Analysis of novel polymers

Following polymerization, crude cross-linked PVPs were pale yellow glasslike materials. Soxhlet extraction and grinding in a planetary ball mill followed by drying in a vacuum oven afforded the novel PVPs as white powders. One of the main properties of the obtained materials was their insolubility in all the usual solvents. The polymers swelled prodigiously in most common organic solvents (dichloromethane, *N,N*-dimethylformamide, methanol, dimethyl sulfoxide) and also in water; the swelling behavior of our novel polymers in comparison with commercial PVP-CL can be retrieved as Supporting information and is available free of charge via the internet at <http://pubs.acs.org>.

Scanning electron microscopy showed that the novel polymers presented a very rough “popcorn-like” appearance, a surface morphology that is similar to commercial PVP-CL, as illustrated in Figure 4. The presence intra-particle pores and expanded surface area make the newly synthesized PVPs interesting materials to investigate in terms of potential application as a drug carrier.

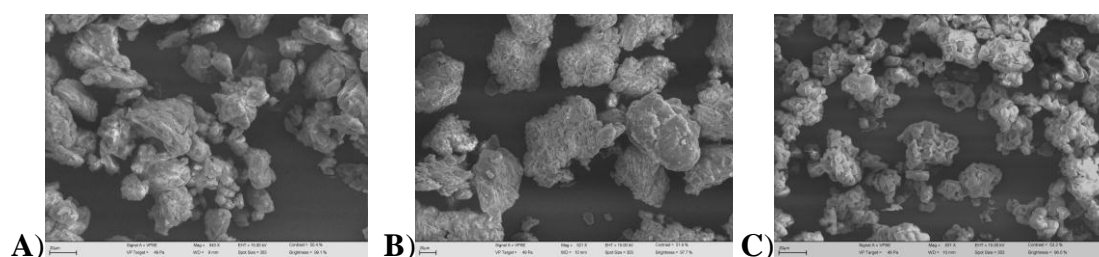


Figure 4. Surface morphology of A) 5 PVP 5%; B) 7 PVP 5%; C) PVP-CL.

FT-IR spectra of all the novel polymers, as well as PVP-CL, were similar. Absorption bands appearing in the region $3000\text{--}2800\text{ cm}^{-1}$ were attributed to the C-H stretching modes, whereas absorption bands at 1420 cm^{-1} were assigned as the C-H bending modes. All spectra featured a strong absorption band at 1670 cm^{-1} as a result of the C=O stretching modes of the *N*-vinylpyrrolidone rings. Another common absorption band exhibited around 1300 cm^{-1} was attributed to a C-N stretching vibration. Spectra can be retrieved as Supporting information and are available free of charge via the internet at <http://pubs.acs.org>.

In characterizing the novel polymers, glass transition temperatures (T_g) were determined and compared with that of PVP-CL. The literature provides several conflicting values for the glass transition temperatures of commercial PVP, ranging from 54°C to 195°C²³⁻²⁵. These deviations are attributed to differences in the structure of the polymer (e.g. linear or cross-linked polymer), the presence absorbed moisture and the method of analysis. Here, glass transition temperatures of the novel PVPs and commercial cross-linked PVP-CL were determined by differential scanning calorimetry. In order to avoid artifacts as a result of prior storage and handling, glass transition temperatures were measured during a second heating cycle; the first heating cycle allowed removal of any residual moisture (which would act as a plasticizer) and erased the effects of thermal history that could obscure the interpretation of T_g . In the analyzed samples, glass transition temperatures were observed over a temperature range, thus the T_g was taken as the midpoint of transition by extrapolation of the enthalpy curve. The data obtained are in Table 2.

Polymer	Mean glass transition temperature (T_g), °C, (n=3, ±SD)
5 PVP 1%	185.5 ± 1.1
5 PVP 2.5%	189.0 ± 1.2
5 PVP 5%	191.0 ± 1.0
7 PVP 1%	182.1 ± 1.1
7 PVP 2.5%	183.7 ± 1.2
7 PVP 5%	185.1 ± 1.1
PVP-CL	195.9 ± 1.0

Table 2. Glass transition temperatures of the novel cross-linked PVPs and commercial cross-linked PVP-CL

All polymers featured similar and high glass transition temperatures, between 182 and 196°C which demonstrates that at room temperature all these polymers are highly stable amorphous solids with relatively low polymer chain mobility's. These high

glass transition temperatures are a desirable property of the novel cross-linked PVPs in terms of their target application as a drug carrier. Some correlation between the structure of the PVPs and glass transition temperature can be seen. For example, T_g increased with higher density of cross-linking in the novel polymers: T_g of 5 PVP 5% > T_g of 5 PVP 2.5% > T_g of 5 PVP 1%. Cross-linking reduces the main-chain mobility of polymers and additionally reduces the distance between polymer chains (i.e. reduced free volume) which would increase the glass transition temperature. Furthermore, it was observed that novel cross-linked PVP containing longer oligoether chains exhibited slightly lower glass transitions than their counterparts with shorter oligoether chain, e.g. T_g of 5 PVP 5% > T_g of 7 PVP 5%. This suggests that the length of the oligoether chain can affect the distance between polymer chains and hence the free volume of polymer. Polymers with longer oligoether chains should exhibit higher free volume than their counterparts with shorter oligoether chains which would decrease the glass transition temperature.

Pharmaceutical evaluation

Example images from scanning electron microscopy of physical mixtures of drug and polymer are in Figure 5. Ibuprofen displays a characteristic ‘needle’ morphology (Figure 5A) and there is clear evidence of these needles in the mixture with PVP-CL (5B). This is consistent with the previous finding of Rawlinson *et al*¹⁰ where, although crystalline to amorphous drug conversion occurred upon mixing and storage with PVP-CL, a significant part of the IB remained in a crystalline form. However for the physical mixtures prepared using the novel polymers, no evidence of ibuprofen crystals could be found when examining the samples over a range of magnifications.

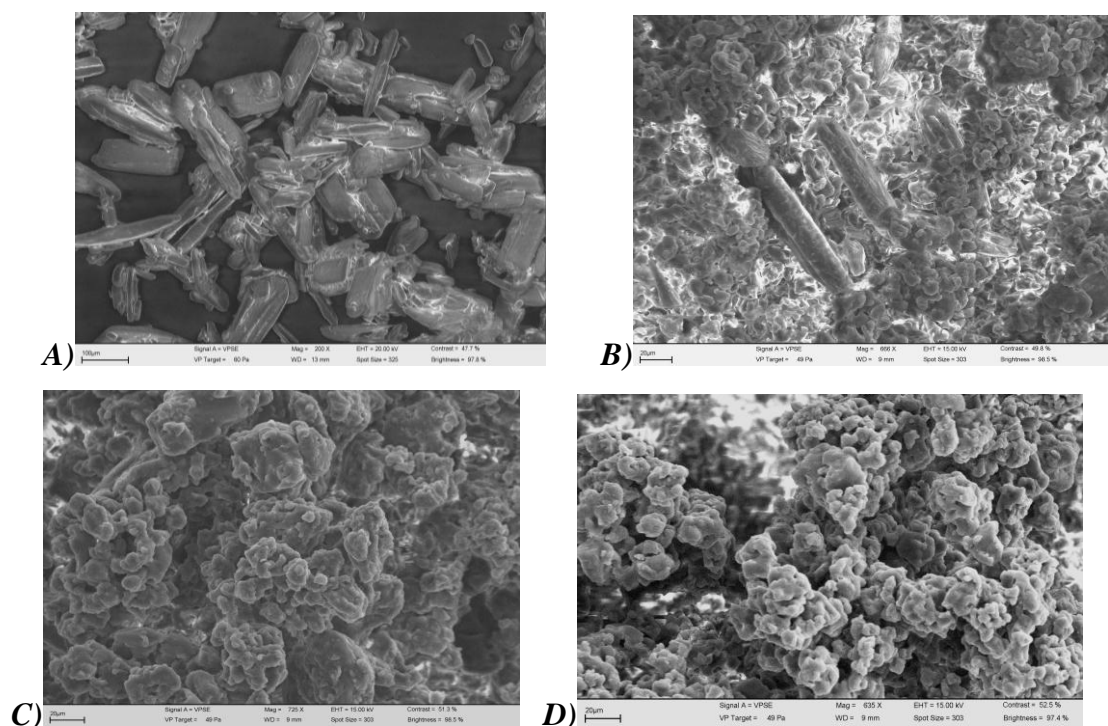


Figure 5. SEM of A) ibuprofen and physical mixtures of ibuprofen with B) PVP-CL, C) 5 PVP 5% and D) 7 PVP 5% (high magnification)

There are two potential explanations for these results. The first is that a ‘macro’ dispersion of the ibuprofen has occurred on mixing with the cross-linked PVPs, that is the ibuprofen particles are hidden, being reduced in size and fully embedded inside polymer cavities; the dimension of the PVP cavities dictates that any crystalline dispersed drug would be significantly size reduced. The images provide no evidence for this type of interaction between the drug and carrier. The second possibility is that a ‘micro’ dispersion has occurred; the highly ordered crystal lattice of ibuprofen has been completely disrupted and the “free” ibuprofen molecules are adsorbed on the polymer particle surfaces or embedded within the polymer in an amorphous form.

The effects of the polymer carriers on the dissolution of IB were investigated for physical mixtures with 30% drug contents. As IB is a weakly acidic drug ($pK_a=5.3$), phosphate buffer at $pH=5.5$ was selected as an intermediate medium which afforded a relatively low drug dissolution rate so allowing greater discrimination of variations in dissolution profiles between IB samples whilst still permitting sink conditions to be maintained. The mean ($n=3$) dissolution profiles of the physical mixtures of IB+PVP are shown in Figure 6, along with the dissolution profile for IB alone. A comparison

of cumulative drug release during the first 15 minutes of dissolution together with that of pure IB is in Table 3. As can be seen from these data, physical mixtures of IB with novel cross-linked PVP increased the dissolution rates compared to the drug alone; the samples with commercial cross-linked PVP exhibited 2-fold increases in IB release during the initial 15 minutes of dissolution testing whereas our novel polymers afforded up to 3-fold increases. The results also revealed that the density of cross-linking of novel PVP affected IB release in the order:

IB+7PVP 5% > IB+7PVP 2.5% > IB+7PVP 1%

IB+5PVP 5% > IB+5PVP 2.5% > IB+5PVP 1%

Dissolution of IB was thus progressively enhanced with increasing PVP cross-linking density. For dissolution profiles of IB where PVPs had the same density of cross-linking, but where the polymers possessed different lengths of oligoether chain (e.g. IB+5PVP 5% and IB+7PVP 5%) the apparent trend of increasing dissolution rate with chain length was not significant.

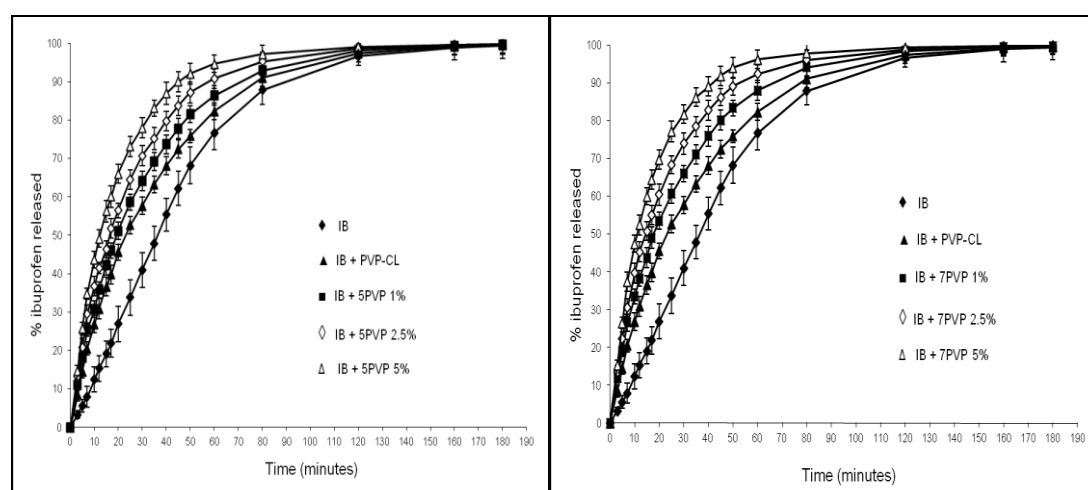


Figure 6. Dissolution profiles of ibuprofen release from: Left; physical mixtures with shorter oligoether linkages (5 PVP series) and Right; physical mixtures with longer oligoether linkages (7 PVP series), $n = 3$, \pm SD.

Sample	Mean % IB released in first 15 minutes (n=3, ±SD)	Increase in initial dissolution, physical mixture/drug alone
IB+5PVP 1%	42.2 ± 2.5	2.21
IB+5PVP 2.5%	46.3 ± 2.2	2.43
IB+5PVP 5%	56.3 ± 2.8	2.95
IB+7PVP 1%	43.7 ± 2.6	2.29
IB+7PVP 2.5%	50.8 ± 2.5	2.66
IB+7PVP 5%	60.0 ± 2.3	3.14
IB+PVP-CL	36.6 ± 2.5	1.92
IB powder alone	19.1 ± 3.4	-

Table 3. Comparison of percentage IB released from the physical mixtures of IB+PVP with that of the pure IB during the first 15 minutes of dissolution testing

The improved dissolution characteristics of physical mixtures, when compared to pure IB, were accompanied by differences in the appearance of the samples in the dissolution medium. Ibuprofen alone floated in an agglomerated form on the surface of the dissolution medium and did not disperse readily throughout the medium even after a few minutes of agitation. However, physical mixtures with all PVP matrices exhibited good dispersion of IB particles (significant deagglomeration) and the physical mixture samples readily “sank” in the dissolution medium and dispersed. These observations provide evidence that the novel cross-linked PVP and commercial cross-linked PVP-CL enhanced the wettability of the IB particles. The mechanism and kinetics of IB release from the polymeric systems was explored. Despite the swellability of the polymers, the dissolution data fitted a first order release profile, consistent with drug release from a porous insoluble matrix.

Differential scanning calorimetry was used to detect changes in the thermal response of IB in physical mixtures compared with a sample of pure IB, to estimate the level of disruption to IB crystallinity in the physical mixture. It is well known that a decrease in drug melting enthalpy could result from dissolution into the polymer matrix but our previous study demonstrated that the thermal results from physical mixtures

correlated well with X-ray diffraction data and so melting enthalpy reductions can be used to quantify crystal disruption¹⁰. Initially, all PVP cross-linked polymers were characterized alone; the traces showed no peaks to indicate defined phase transitions of the PVPs between 22 – 95°C but a broad thermal event was observed, indicative of polymer softening over a wide temperature range. DSC profiles of IB and physical mixtures of IB with PVPs are in Figure 7.

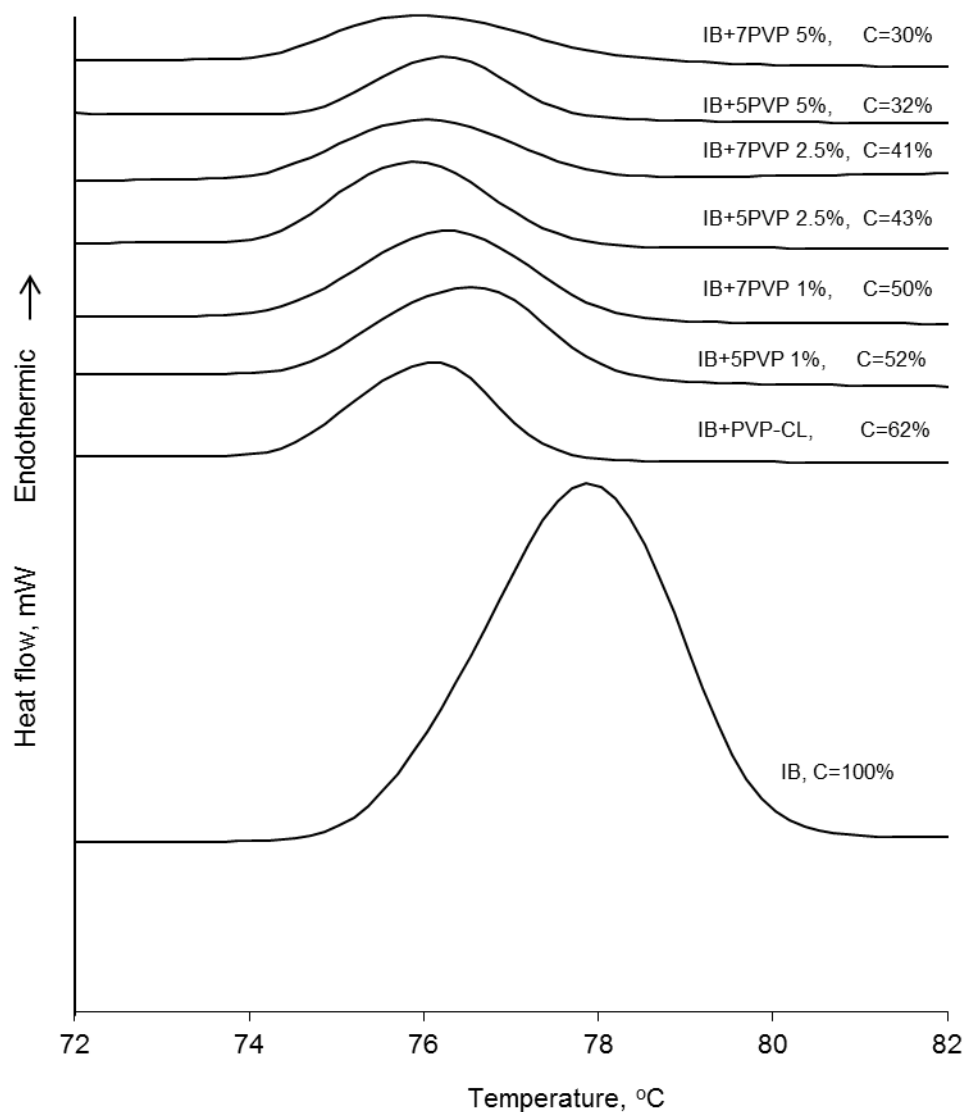


Figure 7. DSC profiles of pure IB and physical mixtures of IB with PVPs. C = estimate of drug crystallinity calculated from enthalpy of melt relative to that of pure ibuprofen, assumed to be 100% crystalline.

The DSC trace of pure IB showed a single relatively sharp endothermic peak with a melting temperature (peak maximum) of 77.9°C and enthalpy of fusion of 118.8 J/g. Significant changes in the peak shape, height-to-width ratio and temperature of melting transition of IB was observed for the drug in physical mixtures; the DSC curves exhibited relatively broad melting endotherms. The widening of the endothermic melting peak and lowering of the onset temperature is indicative of disruption of the IB crystalline structure in the presence of the PVPs. This effect is analogous to the polymers behaving as an impurity for the crystalline IB and provides clear evidence that the cross-linked PVP carriers interact with the drug. Melting points, enthalpies of fusion and estimated drug crystallinity data can be retrieved as Supporting information and are available free of charge via the internet at <http://pubs.acs.org>

Reduction in IB crystallinity in the physical mixture with commercial cross-linked PVP was consistent with literature data⁹. As evident from the DSC analysis, the novel cross-linked polymers appeared to be more effective in disrupting IB crystallinity than commercial cross-linked PVP-CL. Furthermore, the data suggests that the oligoether moieties incorporated into the structure of the novel cross-linked PVP affected the level of disruption IB crystallinity. The most disruptive novel PVPs contained the highest level of oligoether moieties and the highest density of cross-linking. For the same density of cross-linking, the novel polymers containing longer oligoether chains (7 PVP) disrupted crystallinity to a greater extent than their counterparts with shorter oligoether chains (5 PVP).

The increased ability of the PVPs to disrupt IB crystallinity may arise as a result of the presence of oligoether moieties which could provide additional sites for hydrogen bonding interactions. From this, a hypothesis can be proposed that a greater number of hydrogen bonding sites and/or hydrogen bonding sites that may display stronger bonding potential due to neighbor influences will enable a greater degree of disruption of the IB crystal lattice.

In probing molecular interactions between IB and PVP, FT-IR spectra of the PVPs and crystalline IB were used as references for comparison with spectra of the physical mixtures. Functional groups with potential to form hydrogen bonding

interactions within the physical mixture were the carboxyl group of IB ($-\text{C}=\text{O}(\text{OH})$), the carbonyl group of the *N*-vinylpyrrolidone ring ($-\text{C}=\text{O}$) and the ether group in the novel PVP cross-linkers ($-\text{C}-\text{O}$) and so these groups were the focus of the FT-IR studies.

Based on the structures of IB and the PVPs (Figure 8), it can be seen that the polymers can only act as a proton acceptor (through $-\text{C}=\text{O}$ and $-\text{C}-\text{O}$), while IB can only act as a proton donor (through $-\text{OH}$ in the carboxyl group). Thus, hydrogen bonds between IB and PVPs should be detected in the acid carboxyl absorption modes of IB, and PVP carbonyl or C-O absorption modes, depending on the site of interactions.

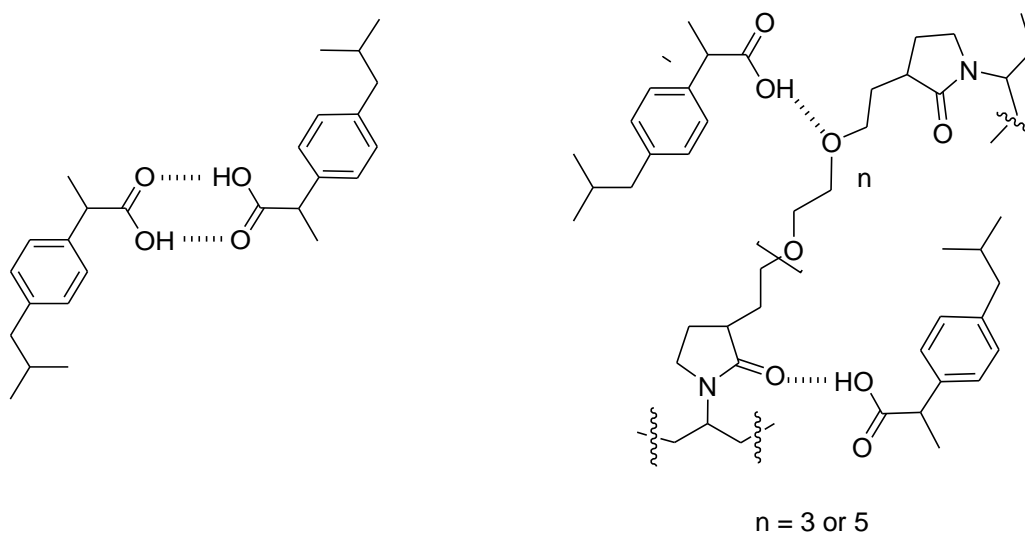


Figure 8. Intra-molecular hydrogen bonding in ibuprofen (dimer) and potential interactions between IB and novel cross-linked PVPs

Literature data¹¹, shows that pure IB forms hydrogen bonded dimers (Figure 8), evidence for which can be seen in the FT-IR spectrum. The hydroxyl ($-\text{OH}$) stretching modes of the carboxylic group appeared in the spectrum of pure IB as a very broad band (in region $3300\text{--}2500\text{ cm}^{-1}$) superimposed on the CH stretching modes (Figure 9). The broad nature of the mode and its position are characteristic of hydrogen-bonded hydroxyl groups and reflected the dimer nature of IB. The FT-IR spectrum of crystalline IB also shows the carbonyl stretching mode at 1710 cm^{-1}

(Figure 9). However, the carbonyl stretching mode of IB dispersed into the novel polymers PVP shifted to higher wavenumbers as a consequence of breaking IB dimers due to interaction with the polymers. The mode appeared at 1723 cm^{-1} for the mixture of IB with commercial cross-linked PVP-CL, whereas for the samples with novel cross-linked PVP the shift was more dramatic, increasing with the higher the contents of the oligoether moieties: IB+7PVP 5% was at 1733 cm^{-1} , IB+7PVP 2.5% at 1729 cm^{-1} and IB+7PVP 1% at 1726 cm^{-1} . Thus the strength of hydrogen bonding interactions between IB and cross-linked PVP was dependent on the type of cross-linker and density of cross-linking. Interestingly, the stretching mode at 1638 cm^{-1} assigned to the hydrogen bonded carbonyl groups of the PVPs remained consistent in intensity relative to the stretching mode at 1672 cm^{-1} which is attributed to the non-hydrogen bonded carbonyl groups of the polymers, suggesting that not the entire polymer was involved in hydrogen bonding interactions with IB.

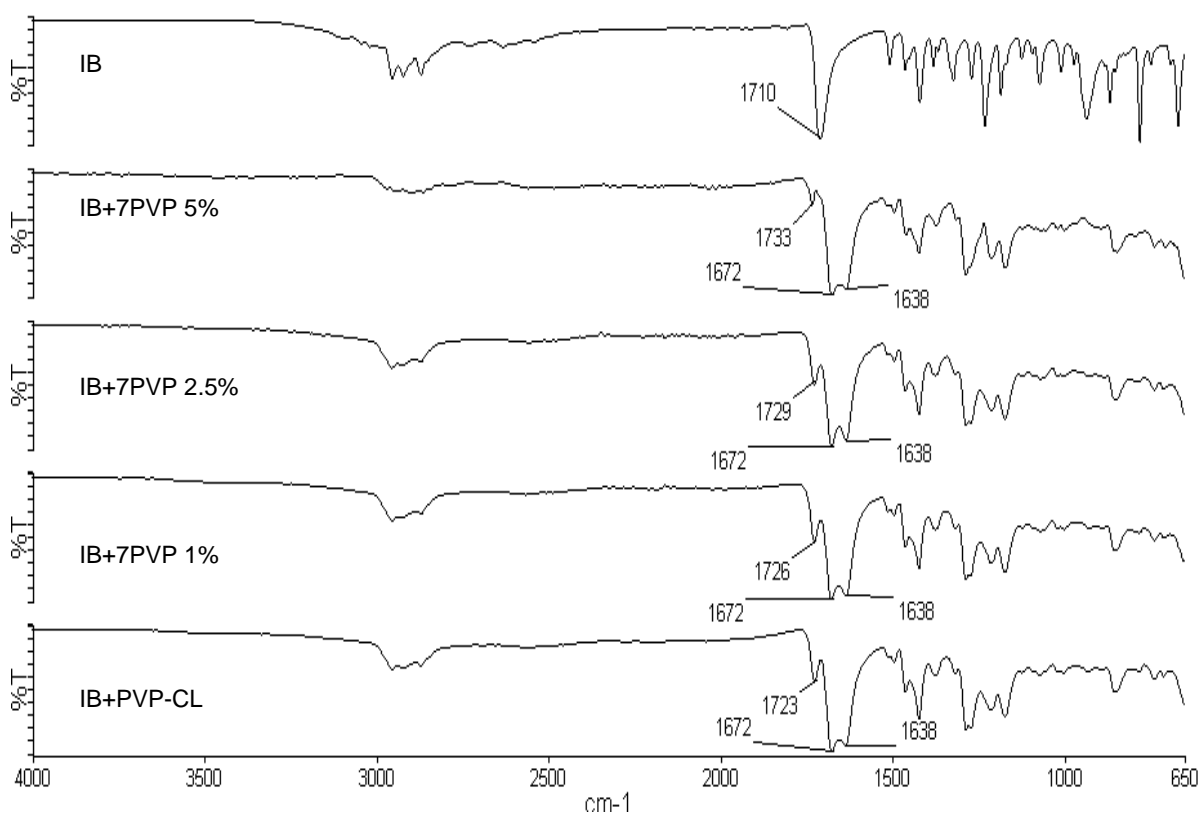


Figure 9 FT-IR spectra of crystalline IB, IB+7PVP 5%, IB+7PVP 2.5%, IB+7PVP 1% and IB+PVP-CL.

FT-IR was also used to probe whether hydrogen bonding occurred between the hydroxyl group of IB and the ether group of the PVP cross-linker in the region 1300-1000 cm^{-1} ; however, these interactions could not be detected, presumably because the amount of the cross-linker was too low to detect any significant changes in the chemical environment. Similar problems were reported in the literature showing the inability of FT-IR to distinguish structural differences between linear PVP and cross-linked PVP^{26, 27}.

As meta-stable systems, amorphous drugs in, for example, solid dispersions tend to recrystallize with time. In contrast, our previous work showed that physical mixtures of IB with PVP-CL continued to disrupt with time, rather than recrystallise¹⁰. Thus, mixtures of ibuprofen with our most cross-linked polymers, which thermal analysis showed had induced greatest disruption of ibuprofen, were examined by powder X-ray diffraction (PXRD) after 20 weeks of storage under nitrogen, alongside samples of polymer and drug alone. The data (Figure 10) shows numerous distinctive diffraction peaks from the crystalline drug alone. In contrast, the polymer carriers showed broad diffuse diffraction patterns characteristic of amorphous materials.

The DSC data (Figure 7) estimated the initial content of crystalline IB in the samples IB+7PVP 5%, IB+5PVP 5% and IB+PVP- 30%, 32% and 62%, respectively. Consistent with our earlier work, after 20 weeks storage under nitrogen, all physical mixtures of IB with our novel and commercial cross-linked PVPs did not show any diffraction peaks from crystalline IB (Figure 10), showing that the reduction in crystallinity induced by the polymers is a kinetic process that continues over a period of weeks. Clearly the interactions between IB and cross-linked PVPs were sufficient to restrict mobility of amorphous IB and inhibit recrystallization, even in the presence of residual crystalline drug. Indeed, it may be that the thermodynamic driver for IB disruption remained and that the kinetics of the process, whilst slowed, continued for an extended time so allowing the 20 weeks samples to appear completely amorphous.

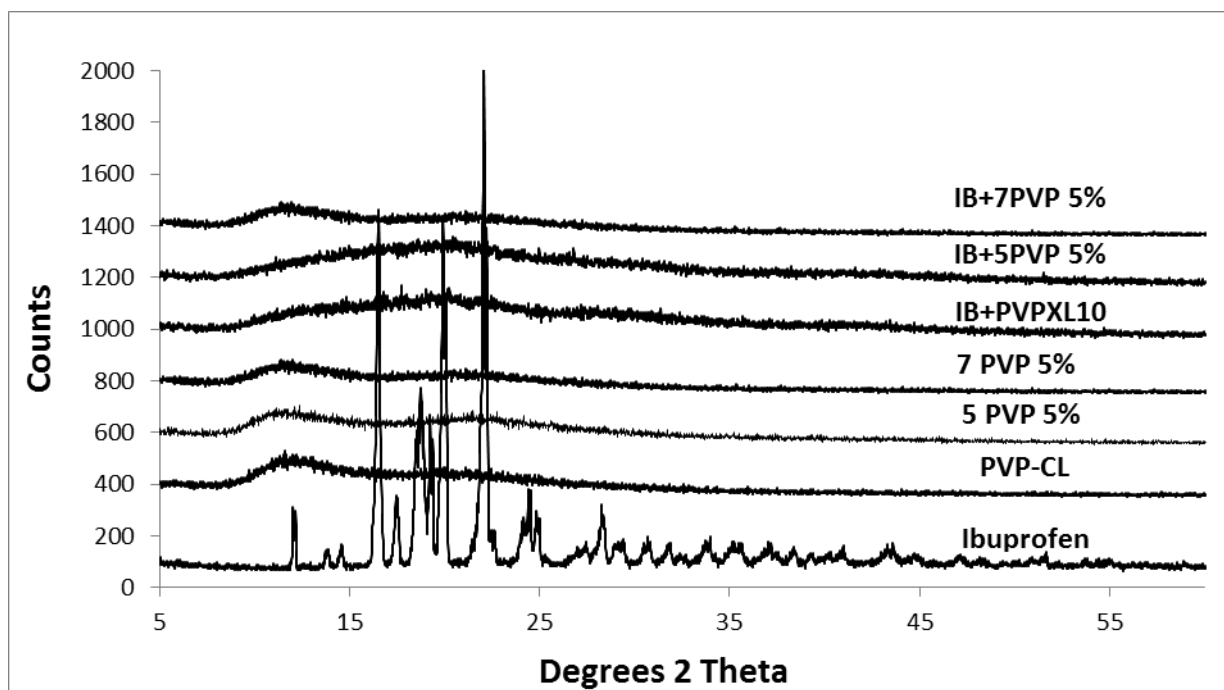


Figure 11. Powder X-ray diffraction patterns of IB, pure PVPs and physical mixtures of IB+PVPs after 20 weeks of storage under nitrogen

From the above, it might be concluded that the thermodynamic driver for IB disruption remained, and that kinetics of the process, whilst slower, continued for an extended time. It is likely that formation of hydrogen bonds in the IB+PVP systems, which is the main driver for disrupting IB crystallinity (as shown above), occurred not only for the “recently” prepared physical mixtures, but proceeded over the time as well. This conclusion could be supported by FT-IR spectra of the “recently” prepared physical mixtures of IB+PVP. The presence of free non-hydrogen bonded carbonyl groups of PVP in the FT-IR spectra indicated that not all hydrogen bonding sites on the PVP were occupied by IB, hence some “PVP hydrogen bonding potential” remained, i.e. bonding sites were unsaturated. Another conclusion drawn from the stability studies was that IB in the physical mixture did not exhibit a tendency to recrystallize, probably because interactions between IB and PVP restricted mobility of the amorphous IB molecules preventing recrystallization. The stability study may also suggest that complete drug conversion to the amorphous state might be achieved through alternative preparation methods that facilitate molecular

mobility and therefore formation of these hydrogen bonds, for example solid dispersions manufactured via solvent or thermal methods.

In addition to the formation of amorphous drug, the PVPs could improve dissolution of poorly-water soluble drugs by improving wetting or the generation of microcrystalline domains. To explore the mechanisms underpinning the enhanced drug dissolution from mixtures, the percentage of IB released within the first 15 minutes (Table 3) can be used as a marker for enhancement in dissolution and can be related to the percentage of drug remaining in the crystalline state as estimated from thermal analysis. The data (Figure 11) shows a linear relationship between amorphous drug fraction and ibuprofen release at 15 minutes. Such a relationship suggests that the predominant mechanism by which the PVPs improved ibuprofen dissolution was via the generation of amorphous drug rather than by other mechanisms described in the literature for dispersed drug in carrier materials, such as increased wettability or particle size reduction.

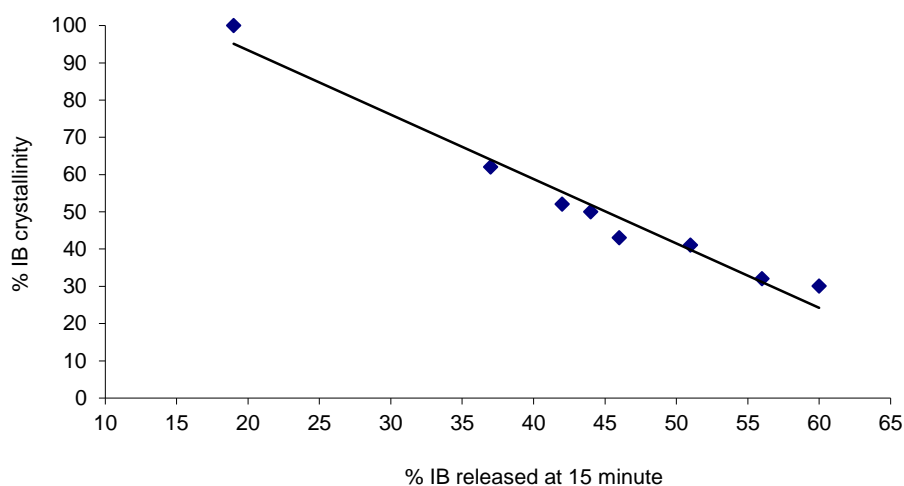


Figure 11 Linear correlation ($R^2 = 0.97$) between percentage IB crystallinity (estimated by thermal analysis) and IB release after 15 minutes

Further, the molecular basis for the generation of amorphous ibuprofen in the mixtures can be directly related to hydrogen bonding between drug and carrier. A

linear relationship was found between the shift in IB carbonyl stretching modes and amorphous content by thermal analysis, which carries forward to a linear relationship between the shift in IB carbonyl stretching mode and percentage drug released at 15 minutes; data can be retrieved as Supporting information and is available free of charge via the internet at <http://pubs.acs.org>.

Our data clearly illustrates the primary role of hydrogen-bonding between ibuprofen and the polymers in stabilizing amorphous drug and by increasing the hydrogen-bonding capacity of our carriers we generate greater crystal disruption with a consequent increase in dissolution rate. However, the thermodynamic driver for this interaction between a crystalline drug and a polymer below its glass transition temperature when gently mixed remains unclear. Polyvinylpyrrolidones are hygroscopic materials and previous work has shown that solid dispersions with this carrier can undergo moisture-mediated phase separation at high relative humidity's^{28, 29}. Typically, water encourages recrystallization of amorphous drugs dispersed in polymeric carriers but in our systems the extensive hydrogen-bonding may inhibit such recrystallization. With linear PVP, drug disruption in mixtures was enhanced at elevated humidities¹⁴ forming solid dispersion type systems. Clearly the presence of moisture (and drug) will plasticize the polymer, reduce its glass transition temperature and increase chain mobility, potentially facilitating interactions between the polymer proton acceptor and drug proton donor sites.

However, we have previously explored the role that moisture may play in mediating interactions between PVP-CL and ibuprofen. Adding 10% water to a simple physical mixture *decreased* the extent of crystal disruption, potentially through water competing for hydrogen-bonding sites in the polymer³⁰. Further, dried PVP-CL (at 60°C, 72h) was mixed with ibuprofen and again extensive crystal disruption was seen by X-ray diffraction³¹. However, the polymer is hygroscopic and had adsorbed 5-6% moisture during the mixing process, a similar moisture content to the starting material. Consequently, experiments were repeated under a vacuum of 700 mmHg and again, ~47% of the ibuprofen crystallinity was lost following simple mixing. The role of external humidity and adsorbed water in facilitating the interactions between PVP-CL and ibuprofen is currently under further investigation.

Finally, ibuprofen has a relatively low melting point (~78°C) which may suggest facile intra-molecular bond breakage to permit hydrogen-bonding with the polymer. It was suggested that enantioselective interactions occurred between ibuprofen and PVP when crystal disruption was compared between the S(+)-enantiomer (melting point ~ 52°C) and the racemate³². Counter-intuitively, when a series of propionic acids were evaluated with increasing melting points (ibuprofen < ketoprofen < flurbiprofen < fenbufen), crystal disruption following 60 minutes of mixing *increased* with increasing melting points³¹. Using a similar series, subsequent work by Gashi et al showed that only ibuprofen spontaneously dispersed in linear PVP, attributed partially to its weak crystalline structure¹³ but on storage at 75% RH the rate of crystal disruption of ibuprofen, ketoprofen, fenbufen and naproxen were similar¹⁴.

Conclusions

Two novel oligoether cross-linking agents were designed, synthesized and characterized. The cross-linkers, tailored to increase the hydrogen bonding capability of polyvinylpyrrolidones, were successfully polymerized with *N*-vinylpyrrolidone to provide six novel PVPs with varying cross-linking oligo chain lengths and cross-link densities. These polymers swell in a range of solvents and have surface characteristics similar to those of commercially available cross-linked PVP. Mixing ibuprofen with the polymers disrupted drug crystallinity and the degree of amorphous conversion was more efficient with the optimized polymers than with commercial PVP-CL. The disruption of crystallinity was directly related molecular interactions

between the drug and polymers, with evidence of ibuprofen dimer disruption and hydrogen bond association between the drug and carriers. Although evidence of disintegrant activity was observed in the swelling studies, the amorphous drug content increased the dissolution rate of ibuprofen from the mixtures, and was the prime mechanism for this enhancement, with no evidence for wetting or microcrystalline drug-based mechanisms operating. The polymers inhibit recrystallization of the drug, even though crystals are present in the initial mixtures, and indeed crystal disruption continued over time.

Acknowledgement

We gratefully acknowledge studentship financial support from Bristol-Myers Squibb for AIN and the Chemical Analysis Facility of the University of Reading for access to characterization equipment. Kenneth Shankland is gratefully acknowledged for his input into the crystallographic studies.

References

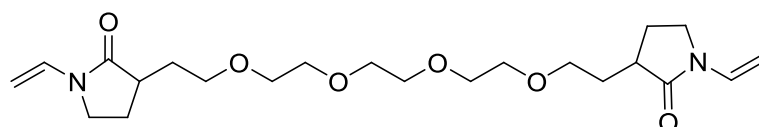
1. Amidon, G.L.; Lennernäs, H.; Shah, V.P.; Crison, J.R. A theoretical basis for a biopharmaceutical drug classification - the correlation of in-vitro drug product dissolution and in-vivo bioavailability. *Pharm. Res.*, **1995**, *12*, 413-420.
2. Kawakami, K., Current status of amorphous formulation and other special dosage forms as formulations for early clinical phases. *J. Pharm. Sci.*, **2009**, *98*, 2875-2885.
3. Craig, D.Q.M., The mechanisms of drug release from solid dispersions in water-soluble polymers. *Int. J. Pharm.*, **2002**, *231*, 131-144.
4. Kaushal, A.M.; Gupta, P.; Bansal, A.K. Amorphous drug delivery systems: molecular aspects, design, and performance. *Crit. Rev. Ther. Drug Carrier Syst.* **2004**, *21*, 133-193.
5. Hancock, B.C.; Zografi, G. Characteristics and significance of the amorphous state in pharmaceutical systems. *J. Pharm. Sci.* **1997**, *86*, 1-12.
6. Mura, P.; Manderioli, A.; Bramanti, G.; Furlanetto, S.; Pinazauti, S. Utilisation of differential scanning calorimetry as a screening technique to determine the compatibility of ketoprofen with excipients. *Int. J. Pharm.*, **1995**, *119*, 71-79.
7. Sekizaki, H.; Danjo, K.; Eguchi, H.; Yonezawa, Y.; Sunada, H.; Otsuka, A. Solid-state interactions of ibuprofen with polyvinylpyrrolidone. *Chem. Pharm. Bull.*, **1995**, *43*, 988-993
8. Rawlinson, C.F.; Williams, A.C.; Timmins, P. Solid-state interactions between ibuprofen and cross-linked polyvinylpyrrolidone within a physical mix. *J. Pharm. Pharmacol.*, **2004**, *56* (Suppl), S34.
9. Williams, A.C.; Timmins, P.; Lu, M.; Forbes, R.T., Disorder and dissolution enhancement: deposition of ibuprofen onto insoluble carriers. *Eur. J. Pharm. Sci.*, **2005**, *26*, 288-294.
10. Rawlinson, C.F.; Williams, A.C.; Timmins, P.T.; Grimsey, I. Polymer-mediated disruption of drug crystallinity. *Int. J. Pharm.*, **2007**, *336*, 42-48.
11. Bogdanova, S.; Pajeva, I.; Nikolova, P.; Tsakovska, I.; Müller, B. Interactions of poly(vinylpyrrolidone) with ibuprofen and naproxen: experimental and modeling studies. *Pharm. Res.*, **2005**, *22*, 806-815.
12. Di Martino, P.; Joiris, E.; Gobetto, R.; Masic, A.; Palmieri, G.F.; Martelli, S. Ketoprofen-poly(vinylpyrrolidone) physical interaction. *J. Cryst. Growth*, **2004**, *265*, 302-308.
13. Gashi, Z.; Censi, R.; Malaj, L.; Gobetto, R.; Mozzicafreddo, M.; Angeletti, M.; Masic, A.; Di Martino, P. Differences in the interaction between aryl propionic acid derivatives and poly(vinylpyrrolidone) K30: A multi-methodological approach. *J. Pharm. Sci.*, **98**, 4216-4228.
14. Malaj, L.; Censi, R.; Mozzicafreddo, M.; Pellegrino, L.; Angeletti, M.; Gobetto, R.; Di Martino, P. Influence of relative humidity on the interaction between different aryl propionic acid derivatives and poly(vinyl)pyrrolidone K30: Evaluation of the effect on drug bioavailability. *Int. J. Pharm.*, **2010**, *398*, 61-72

15. White, L.A., Hoyle, C.E., Jonsson, S. and Mathias, L.J.; Synthesis of 3-alkylated-1-vinyl-2-pyrrolidones and preliminary kinetic studies of their photopolymerizations, *Polymer*, 1999, **40**, 6597-6605.
16. White, L.A., Hoyle, C.E., Jonsson, S. and Mathias, L.J.; Bulk free-radical photopolymerizations of 1-vinyl-2-pyrrolidinone and its derivatives, *J. Polym. Sci., A Polym. Chem.*, **2002**, 40, 694-706.
17. Teberekidis, V.I.; Sigalas, M.P. Theoretical study of hydrogen bond interactions of felodipine with polyvinylpyrrolidone and polyethyleneglycol. *J. Mol Struct: THEOCHEM.*, **2006**, 803, 29–38.
18. Greenley, R.Z.; Recalculation of some reactivity ratios, *J. Macromol. Sci. Chem.*, **1980**, A14 (4), 445-515.
19. Bencini, M.; Ranucci, E.; Ferruti, P.; Oldani, C.; Licandro, E.; Maiorana, S. Synthesis of 3,3-di(ethoxycarbonyl)-1-vinylpyrrolidin-2-one and determination of its reactivity ratios with 1-vinylpyrrolidin-2-one. *Macromolecules*, **2005**, 20, 8211-8219.
20. Engström, J.U.A., Lindgren, L.J. and Helgee, B.; Synthesis of novel monomers and copolymers from 1-vinylpyrrolidin-2-one: Attractive materials for drug delivery systems? *Macromol. Chem. Physic.*, **2006**, 207, 536-544.
21. Engström, J.U.A., Helgee, B., Sung, S.D. and Bergbreiter, D.E.; Novel densely alkylated hydroxyl-functional polyvinylpyrrolidone showing phase-selective solubility, *Macromol. Chem. Physic.*, **2006**, 207, 1062-1069.
22. Engström, J.U.A. and Helgee, B.; Hydrophilic polymer supports for solid-phase synthesis: hydroxyl-functional beads of poly(vinylpyrrolidone), *J. Comb. Chem.*, **2006**, 8, 355-360.
23. Hamura, T. and Newton, M.J.; Interaction between water and poly(vinylpyrrolidone) containing polyethylene glycol, *J. Pharm. Sci.*, **1999**, 88, 1228 -1233.
24. Oksanen, C.A. and Zograf, G.; The relationship between the glass transition temperature and water vapor absorption by poly(vinylpyrrolidone), *Pharm. Res.*, **1990**, 7, 654-657.
25. Yoshioka, M., Hancock, B.C. and Zograf, G.; Inhibition of indomethacin crystallization in poly(vinylpyrrolidone) coprecipitates, *J. Pharm. Sci.*, **1995**, 84, 983-986.
26. Haaf, R. and Sanner, A.; Polymers of N-Vinylpyrrolidone: synthesis, characterization and uses, *Polym. J.*, **1985**, 17, 143-152.
27. Bühler, V.; *Kollidon: Polyvinylpyrrolidone Excipients for the Pharmaceutical Industry*, **2008**, Ninth Revised Edition, BASF
28. Rumondor, A.C.F.; Marsac, P.J.; Stanford, L.A.; Taylor, L.S.; Phase behavior of poly(vinylpyrrolidone) containing amorphous solid dispersions in the presence of moisture. *Mol. Pharmaceutics*, **2009**, 6, 1492-1505.
29. Rumondor, A.C.F.; Taylor, L.S.; Effect of polymer hygroscopicity on the phase behavior of amorphous solid dispersions in the presence of moisture. *Mol. Pharmaceutics*, **2010**, 7, 477-490.

30. Lu, M.; "Improving poorly water-soluble drug delivery through stabilised amorphous systems. PhD Thesis, University of Bradford, West Yorkshire, UK., **2002**.
31. Rawlinson, C.F.; "Polymer-mediated disordering and dissolution enhancement of poorly water-soluble drugs. PhD Thesis, University of Bradford, West Yorkshire, UK., **2006**.
32. Ivanov, I.T.; Tsokeva, Z.; Effect of chirality on PVP/drug interaction within binary physical mixtures of ibuprofen, ketoprofen and naproxen: A DSC study, *Chirality*, **2009**, 21, 719-727.

Analytical characterization of materials:

3,3'-(3,6,9,12-tetraoxatetradecane-1,14-diyl)bis(1-vinyl-2-pyrrolidinone)



TLC $R_f = 0.29$ (aluminium sheets coated with Merck silica gel 60 F₂₅₄; ethyl acetate/hexane 9:1 v/v).

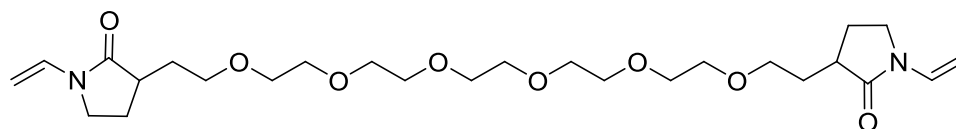
¹H NMR (250 MHz, CDCl₃) δ 1.60-1.71 (2H, m, 2 \times -CHCH(H)CH₂O-), 1.80 (2H, app. dq, $J=9.0, 12.8$ Hz, 2 \times -CH(H)CH₂N-), 2.13-2.25 (2H, m, 2 \times -CHCH(H)CH₂O-), 2.28-2.41 (2H, m, 2 \times -CH(H)CH₂N-), 2.65 (2H, app. dq, $J=4.9, 9.0$ Hz, 2 \times -CH-C=O), 3.38 (2H, app. dt, $J=8.1, 10.0$ Hz, 2 \times -CH₂N-), 3.51 (2H, app. dt, $J=2.9, 9.4$ Hz, 2 \times -CH₂N-), 3.56-3.68 (16H, m, 2 \times -CHCH₂CH₂O-(CH₂)₂O-CH₂-), 4.40 (2H, app. d, $J=16.0$ Hz, 2 \times -CH=CH₂), 4.44 (2H, app. d, $J=9.0$ Hz, 2 \times -CH=CH₂), 7.09 (2H, dd, $J=9.1, 16.0$ Hz, 2 \times -CH=CH₂).

¹³C NMR (62.5 MHz, CDCl₃) δ 24.8 (2 \times -CH₂CH₂N-), 31.0 (2 \times -CHCH₂CH₂O-), 39.8 (2 \times -CH-C=O), 42.9 (2 \times -CH₂N), 69.1 (2 \times -CHCH₂CH₂O-), 70.1 (2 \times -CH(CH₂)₂OCH₂CH₂-), 70.6 (2 \times -CH(CH₂)₂OCH₂CH₂-OCH₂-), 94.2 (2 \times -CH=CH₂), 129.5 (2 \times -CH=CH₂), 175.0 (2 \times -C=O).

IR (CH₂Cl₂, cm⁻¹) 2868, 1697, 1629, 1481, 1452, 1424, 1387, 1327, 1264, 1110, 1033, 979, 845.

CI-MS [MH]⁺ calculated for C₂₂H₃₇N₂O₆: 425.2651, found: 425.2646.

3,3'-(3,6,9,12,15,18-hexaoxaicosane-1,20-diyl)bis(1-vinyl-2-pyrrolidinone)



TLC $R_f = 0.25$ (aluminium sheets coated with Merck silica gel 60 F₂₅₄; ethyl acetate/hexane 9:1 v/v).

¹H NMR (250 MHz, CDCl₃) δ 1.57-1.72 (2H, m, 2 \times -CHCH(H)CH₂O-), 1.80 (2H, app. dq, $J=9.0, 12.8$ Hz, 2 \times -CH(H)CH₂N-), 2.12-2.25 (2H, m, 2 \times -CHCH(H)CH₂O-), 2.28-2.41 (2H, m, 2 \times -CH(H)CH₂N-), 2.65 (2H, app. dq, $J=4.9, 9.0$ Hz, 2 \times -CH-C=O), 3.38 (2H, app. dt, $J=8.1, 10.1$ Hz, 2 \times -CH₂N-), 3.51 (2H, app. dt, $J=3.0, 10.1$ Hz, 2 \times -CH₂N-), 3.57-3.66 (24H, m, 2 \times -CHCH₂CH₂O-(CH₂CH₂O)₂-CH₂-), 4.40 (2H, app. d, $J=16.0$ Hz, 2 \times -CH=CH₂), 4.44 (2H, app. d, $J=9.0$ Hz, 2 \times -CH=CH₂), 7.09 (2H, dd, $J=9.0, 16.0$ Hz, 2 \times -CH=CH₂).

¹³C NMR (62.5 MHz, CDCl₃) δ 24.8 (2 \times -CH₂CH₂N-), 31.0 (2 \times -CHCH₂CH₂O-), 39.8 (2 \times -CH-C=O), 42.9 (2 \times -CH₂N), 69.1 (2 \times -CHCH₂CH₂O-), 70.1 (2 \times -CH(CH₂)₂OCH₂CH₂-), 70.6 (2 \times -CH(CH₂)₂OCH₂CH₂O(CH₂)₂OCH₂-), 94.2 (2 \times -CH=CH₂), 129.5 (2 \times -CH=CH₂), 175.1 (2 \times -C=O).

IR (CH₂Cl₂, cm⁻¹) 2920, 2868, 1697, 1629, 1484, 1452, 1424, 1384, 1324, 1267, 1108, 1033, 979, 848.

CI-MS [MH]⁺ calculated for C₂₆H₄₅N₂O₈: 513.3176, found: 513.3180.

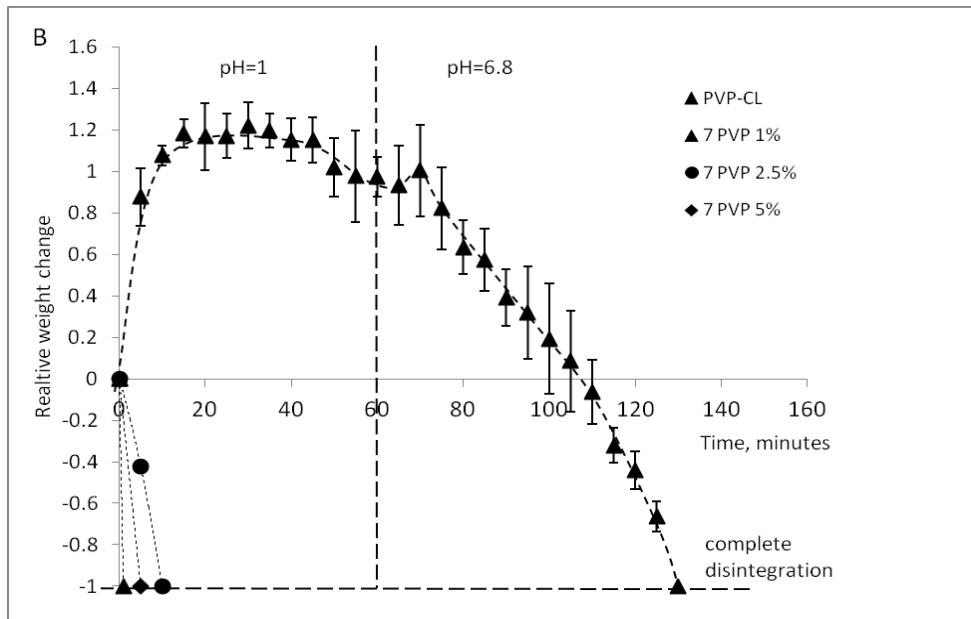
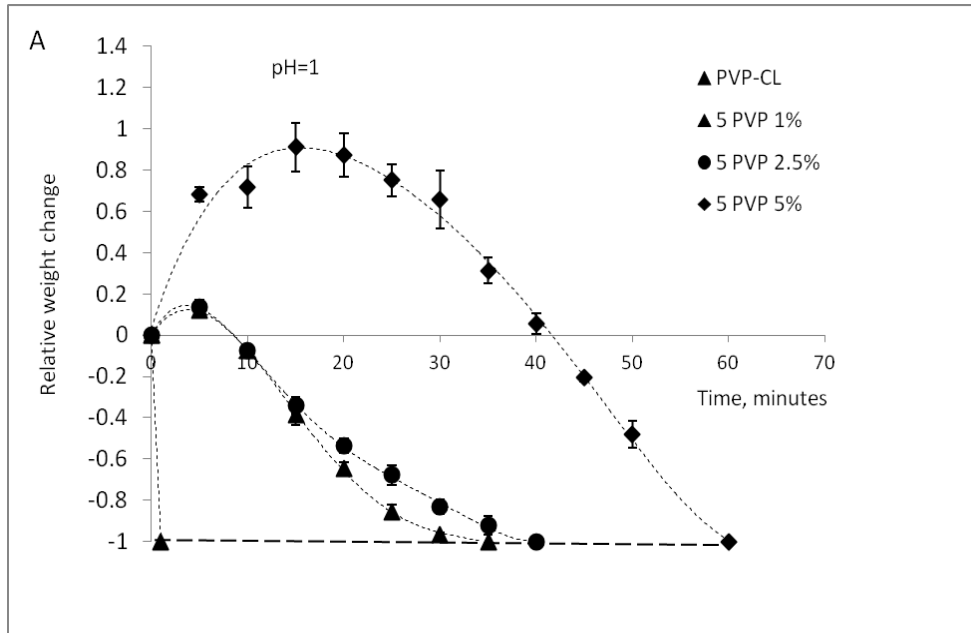
Swelling behaviour of tablets of PVP-CL and novel PVP.

Tablets of our polymers and commercial PVP-CL were prepared by direct compression of the powders on a single punch tablet press (RIVA Minipress MII, Argentina). Tablets were weighted and submerged into buffer solution simulated gastric fluid (pH=1) (British Pharmacopoeia, 2011) at 37 °C for 1 hour, then intact tablets were transferred into artificial gastric solution (pH=6.8) (US Pharmacopeia). Tablets were withdrawn from media at 5 minutes intervals, blotted and weight recorded. Water uptake was calculated by:

$$\text{Relative weight change} = \frac{W_h - W_i}{W_i}$$

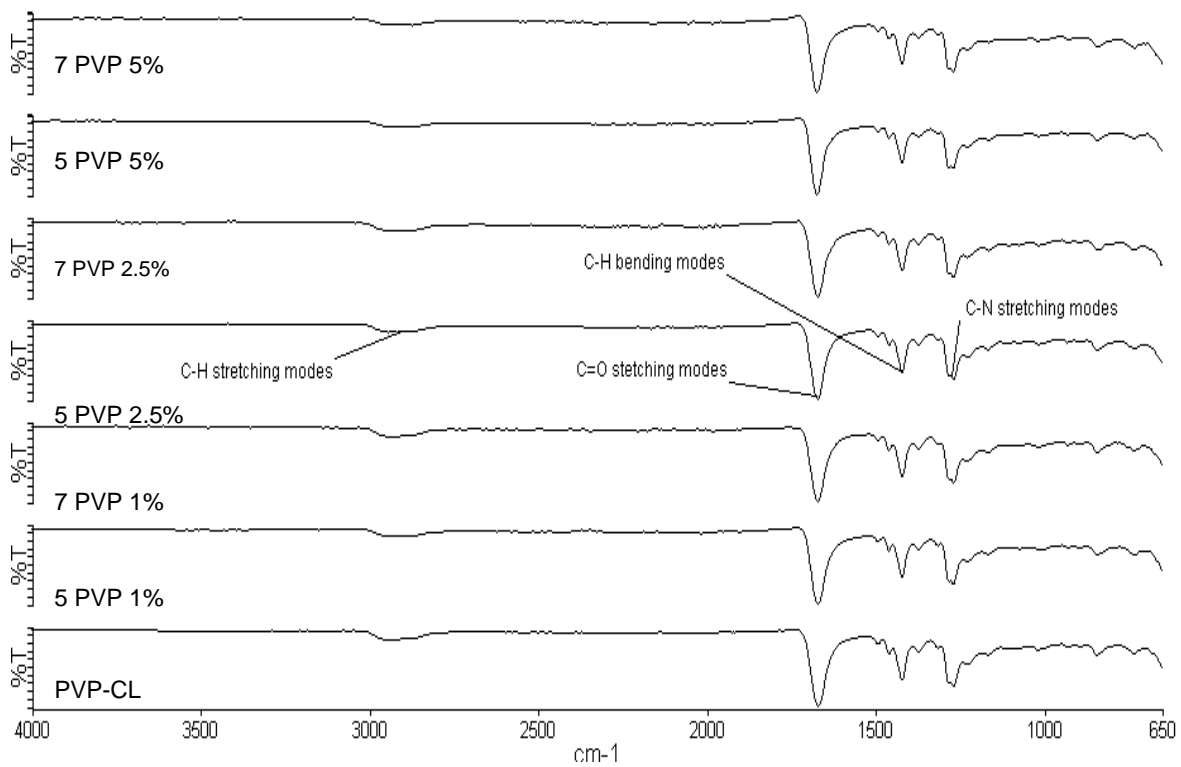
where W_i and W_h are the initial weight and the weight of the hydrated tablet, respectively.

Commercial PVP-CL tablets rapidly disintegrated at pH1.0. The 5 PVP series of polymers swelled significantly at pH 1.0 with the greatest degree of swelling seen for the most highly cross-linked polymer, 5 PVP 5%. However, all tablets disintegrated within 1 hour and so could not be transferred to the second buffer at pH 6.8. Such swelling behaviour indicates that these novel polymers would be useful for rapid tablet disintegration and consequently rapid absorption in the upper G.I. tract. In contrast, the longer cross-linker-containing polymers showed varied behaviour in the different buffers; the more highly cross-linked systems 7 PVP 2.5% and 7 PVP 5% did not swell at pH 1.0 and disintegrated rapidly, as was the case for the commercial PVP-CL. However, 7 PVP 1%, containing the lowest cross-link density, did swell prodigiously at pH1.0 and the disintegrated relatively slowly when transferred to pH 6.8, suggesting that the polymer could be a valuable “superdisintegrant” for drug delivery throughout the gastrointestinal tract. Overall, these data present a complicated relationship between linker chain length, cross-linking density, and swelling and disintegrant properties of the novel polymers.



Swelling behaviour of tablets of polyvinylpyrrolidones showing A) 5 PVP series containing shorter cross-linker and B) 7 PVP series containing longer cross-linker.

FT-IR spectra of novel cross-linked PVPs and commercially available PVP-CL

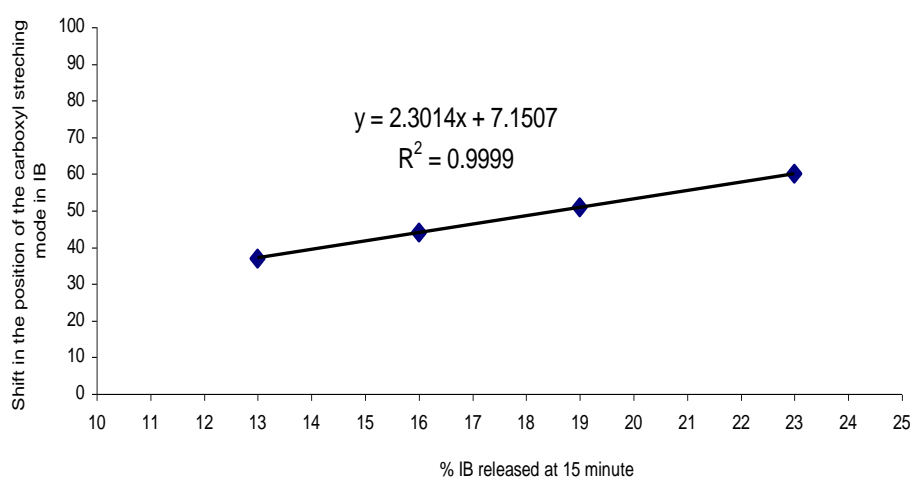


Summary of thermal analysis data for drug:polymer mixtures showing enthalpy of fusion for IB in the mixture and an estimate of drug crystallinity, n=3, ±SD

Sample	Fusion Enthalpy (J/g), n=3, ±SD	Theoretical fusion enthalpy (J/g)	Crystallinity (%), n=3, ±SD
IB	118.8		100
IB+PVP-CL	22.2 ± 1.0	118.8 x 0.3 = 35.6	62 ± 2.8
IB+7PVP 5%	10.6 ± 1.2		30 ± 3.2
IB+5PVP 5%	11.4 ± 1.0		32 ± 2.8
IB+7PVP 2.5%	14.6 ± 1.1		41 ± 3.0
IB+5PVP 2.5%	15.3 ± 0.9		43 ± 2.7
IB+7PVP 1%	17.9 ± 1.2		50 ± 3.3
IB+5PVP 1%	18.6 ± 0.9		52 ± 2.7

Relationship between ibuprofen released at 15 minutes and alteration to the carbonyl stretching mode of ibuprofen

Samples	% IB released at 15 minute	Shift in the position of the carboxyl stretching mode in IB (cm⁻¹)
IB+7PVP 5%	60	23
IB+7PVP 2.5%	51	19
IB+7PVP 1%	44	16
IB+PVP-CL	37	13



Relationship between alteration to carbonyl stretching mode of ibuprofen and the percentage of amorphous ibuprofen formed in physical mixtures with PVPs

Samples	Shift in the position of the carboxyl stretching mode in IB (cm⁻¹)	% amorphous IB
IB+7PVP 5%	23	70
IB+7PVP 2.5%	19	59
IB+7PVP 1%	16	50
IB+PVP-CL	13	38

